Article

Modelling a Switching Process of IGBTs with Influence of Temperature Taken into Account †

Paweł Górecki and Krzysztof Górecki *

Department of Marine Electronics, Gdynia Maritime University, 81-225 Gdynia, Poland; p.gorecki@we.umg.edu.pl
* Correspondence: k.gorecki@we.umg.edu.pl

† This paper is an extended version of our paper published in 24th International Workshop on Thermal Investigations of ICs and Systems Therminic 2018, Kista, 164 40 Stockholm, Sweden, 26–28 September 2018, doi:10.1109/THERMINIC.2018.8592873.

Received: 1 April 2019; Accepted: 14 May 2019; Published: 18 May 2019

Abstract: In this article the problem of modelling a switching process of Insulated Gate Bipolar Transistors (IGBTs) in the SPICE software is considered. The new form of the considered transistor model is presented. The model includes controlled voltage and current sources, resistors and voltage sources. In the model, influence of temperature on dc and dynamic characteristics of the IGBT is taken into account. A detailed description of the dynamic part of this model is included in the article and some results of experimental verification are shown. Verification is performed for a transistor IRG4PC40UD by International Rectifier. The presented results of computations and measurements show clearly influence of temperature on on-time and off-time, and additionally switching energy losses are observed. Moreover, the results of investigations performed with the use of the new model are compared to the results of computations performed with classical models of the considered device given in the literature. It is proved that the new model makes it possible to obtain a better match to the results of measurements than the considered models described in the literature.

Keywords: power semiconductor devices; IGBT; modelling; transient analysis; SPICE; switching; thermal phenomena

---

1. Introduction

Insulated Gate Bipolar Transistors (IGBTs) belong to the group of power semiconductor devices [1]. They are commonly used as electronic switches in power electronic applications [2–4]. In a process of designing such circuits computer simulations are typically realized.

In order to perform reliable simulations of an electronic circuit, proper software and accurate models of all electronic components included in this circuit are indispensable. One of the most popular software for a computer analysis of electronic and power electronic circuits is SPICE [2,4–10]. In this software, models of many semiconductor devices, including a model of the IGBT, are built-in. Additionally, in many papers, e.g., [11–18], different forms of IGBT models are described. Of course, these models differ from one another by accuracy and the form. In the mentioned models, physical phenomena occurring in the IGBT could be described using equations of different forms.

In the authors' previous papers [16,17,19] accuracy of selected models of the considered transistor given in the literature are analysed and new forms of dc model of the considered transistor correctly describing influence of temperature on its dc characteristics are presented. The results of computations and measurements shown in the cited papers prove that the considered literature models correctly describe dc characteristics of the considered transistor at room temperature only, whereas visible

differences between the results of computations and measurements can be obtained at a high temperature value (over 100 °C) and in the sub-threshold range of operation.

Typically, IGBTs are used as electronic switches operating in switch-mode power converters [2–4,20–22]. In such converters dynamic properties of the considered transistor are very important. These properties limit the value of switching frequency and they are characterised by such parameters as, e.g., by turn-off and turn-on times [3]. Values of these parameters change when temperature changes [23,24].

In this paper, which is an extended version of the conference paper [25], the problem of modelling dynamic properties of the IGBT is considered. Properties of selected literature models of the IGBT and their usefulness for proper computations of waveforms of terminal voltages and currents of this transistor during a switching process in a wide range of temperature are investigated. A new dynamic model of the IGBT for SPICE is proposed and its correctness is verified experimentally for different values of temperature.

In Section 2 the elaborated model is described, whereas in Section 3 some results of computations performed with the use of the new model and literature models as well as the results of measurements are shown and discussed.

2. Model Description

On the basis of the previously formulated by the authors dc model of the IGBT dedicated for the SPICE software [16], a new dynamic model of this device is formulated. In the new dynamic model controlled current sources describing currents flowing through parasitic capacitances of the considered transistor are added. In some papers, e.g., [1,11,26] the IGBT is typically modelled using the network representation of this device shown in Figure 1. As it is visible in the structure of the IGBT, three components can be distinguished: The MOSFET, the BJT and the diode.

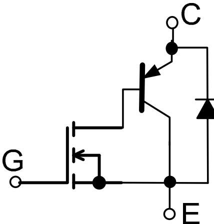

Figure 1. Network representation of the typical structure of the Insulated Gate Bipolar Transistor (IGBT).

On the basis of this classical IGBT structure presented in Figure 1 a new dynamic model taking into account parasitic capacitances is elaborated. The network representation of the new model, based on the conception presented in Figure 1, is shown in Figure 2.

In Figure 2, electronic components describing dc characteristics of the IGBT are marked with yellow colour and labelled as a dc model. In turn, controlled current sources $\mathrm{G_{CGE}}$, $\mathrm{G_{CCE}}$ and $\mathrm{G_{CGC}}$ model currents flowing through internal capacitances C_{GE}, C_{CE} and C_{GC}, respectively, of the transistor. In analytical formulas describing the considered controlled current sources influence of temperature on the value of the mentioned capacitances is taken into account.

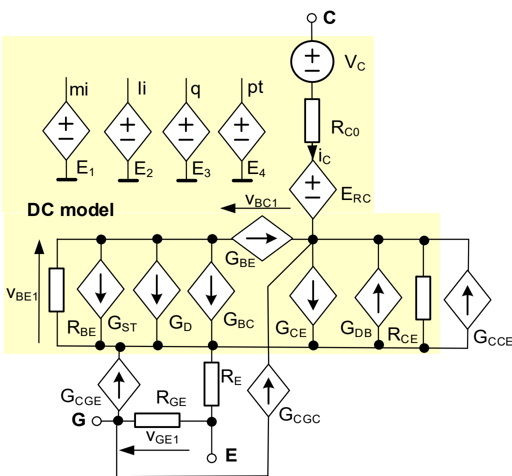

Figure 2. Network representation of the elaborated dynamic model of the IGBT.

In the dc model of the IGBT, drain current of the internal MOS structure is represented by two controlled current sources: G_D describing channel current of the MOS transistor and G_{ST} modelling the sub-threshold component of this current. To compute the values of currents and voltages in the model of the internal MOS structure, auxiliary controlled voltage sources (E_1, E_2, E_3 and E_4) are indispensable.

The controlled current source G_{BE} represents current flowing between the base and the emitter of the bipolar transistor contained in the structure of the modelled transistor. In turn, the controlled current source G_{BC} describes current flowing between the base and the collector of the bipolar transistor contained in the modelled IGBT.

The controlled current source G_{CE} models the main current of the IGBT. The controlled current source G_{DB} models dc characteristic of the diode. All the equations used to describe all the mentioned controlled current sources are described and discussed in paper [16].

In order to model electric inertia of the IGBT controlled current sources G_{CGE}, G_{CCE} and G_{CGC} are used. The mentioned current sources model current flowing through parasitic capacitances of the transistor: C_{GE}, C_{CE} and C_{GC}, respectively. These currents are described with formulas presented below. Capacitance between the collector and the emitter is described by formula of the form analogous to formula describing p-n junction capacitance. Because this junction does not rapidly change into the forward mode, in the equation describing this capacitance the diffusive component is omitted, but influence of temperature on this capacitance is described by following formula:

$$C_{CE} = C_{CE0} \cdot \left(1 + \frac{V_{CE}}{V_j}\right)^{-M_j \cdot (1 + r \cdot (T_j - T_0))} \tag{1}$$

where V_{CE} marks the collector emitter voltage, C_{CE0}—output capacitance of the IGBT at zero voltage on the diode, V_j—built-in potential of reverse diode, M_j—parameter describing the doping profile of the junction, r—the temperature coefficient of parameter M_j, T_j—internal temperature of the IGBT, T_0—reference temperature.

Capacitance between the gate and the emitter of the transistor is described by the following spline:

$$\begin{aligned} C_{GE} &= C_{GE0} \cdot w + x \cdot \left(T_j - T_0\right) + \\ &+ \begin{cases} 0 \; if \; V_{GE} < V_{GE\min} + V_{C1E} \\ C_{0x} \cdot k_1 \cdot (C_{G1} \cdot V_{GC1} + C_{G2}) \; if \; V_{GE\min} + V_{C1E} < V_{GE} \leq V_{GE\max} + V_{C1E} \\ C_{0x} \; if \; V_{GE} > V_{GE\max} + V_{C1E} \; and \; V_{C1E} < 0 \\ C_{0x} \cdot \left[u \cdot \left(T_j - T_0\right) + 0.75 \cdot \left(\frac{V_{GC1}}{2 \cdot V_{GE} + V_{C1E}}\right)^2\right] if \; V_{GE} > V_{GE\max} + V_{C1E} \; and \; V_{C1E} \geq 0 \end{cases} \end{aligned} \tag{2}$$

where C_{0x} is capacitance dependent on thickness of the layer of oxide under the gate t_{OX}, w—width of the channel of the MOS structure, C_{GE0}—capacitance per unit of channel widths between the gate and the emitter, V_{GEmax}, V_{GEmin}, C_{G1}, C_{G2}, x, u and k_1—other parameters of the model, whereas V_{GE} and V_{C1E} are voltages marked in Figure 2.

Capacitance C_{ox} occurring in Equation (2) is given by formula of the form [8,27]:

$$C_{ox} = \frac{\varepsilon_0 \cdot \varepsilon_{ox} \cdot L \cdot w}{t_{OX}} \tag{3}$$

where L denotes the length of the channel of the MOS structure, ε_0 is dielectric permeability of free air, and ε_{ox} relative dielectric permeability of silicon oxide.

Capacitance between the gate and the collector is described by the dependence of the form:

$$C_{GC} = C_2 \cdot \frac{i_C \cdot q}{k \cdot T_j} + \begin{cases} C_1 \cdot w \; if \; V_{GC1} < V_{GC\min} + e \cdot \left(T_j - T_0\right) \\ \left[C_{GD0} + y \cdot \left(T_j - T_0\right)\right] \cdot w \cdot \left(1 + \frac{V_{C1E}}{V_{jC}}\right)^{-M_{j2} + n \cdot (T_j - T_0)} if \; V_{GC1} \geq V_{GC\min} + e \cdot \left(T_j - T_0\right) \end{cases} \tag{4}$$

where C_{GD0} is capacitance per the unit of channel width between the gate and the drain on the unit of the channel width, C_1, C_2, y, e, n, V_{GCmin}—other parameters of the model, M_{j2}—parameter describing the doping profile of this junction, V_{jC}—potential of the base-emitter junction, q—electron charge k—the Boltzmann constant, i_C—collector current.

In practice, in order to model each of these capacitances, the use of a subcircuit shown in Figure 3 is needed.

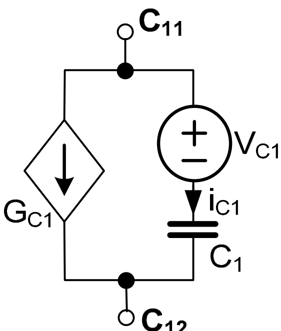

Figure 3. Manner of modelling internal capacitances of the transistor.

This subcircuit consists of linear capacitor C_1 of the fixed value of capacitance, voltage source V_{C1} of the zero value and the controlled current source G_{C1}. The voltage source V_{C1} is used to monitor the value of current i_{C1}, which is proportional to time derivatives of voltage on the current source G_{C1} and on the capacitor C_1. The current flowing through the controlled current source G_{C1} modelling parasitic capacitance C_X is given by the following formula:

$$I_{GC1} = \frac{C_x - C_1}{C_1} \cdot i_{C1} \tag{5}$$

In the presented dynamic model of the IGBT output currents of the considered controlled current source (G_{CCE}, G_{CGE} and G_{CGC}) describing current flowing through parasitic capacitances of the IGBT are described by Equation (5), in which capacitance C_x is equal to the appropriate capacitances described with Equations (1)–(4).

3. Results of Computations and Measurements

In order to verify usefulness of the worked out dynamic IGBT model many computations and measurements of waveforms of collector current while switching-on and switching-off this device were performed. Measurements were realised in the measurement set-up shown in Figure 4.

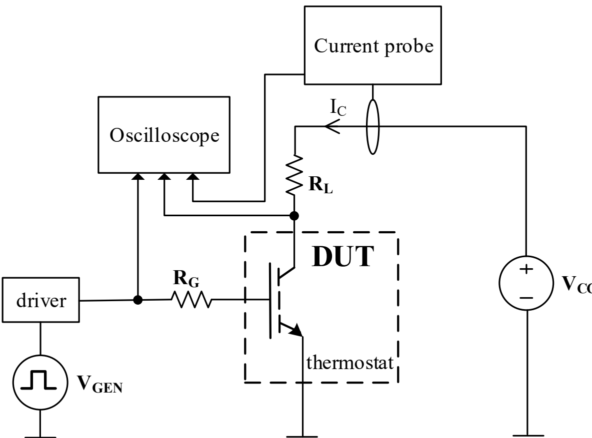

Figure 4. Diagram of a set-up to measure waveforms of voltage and currents of the IGBT while switching.

In the presented measurement set-up, voltage source V_{CC} feeds the collector of the investigated device. The control signal is generated by the function generator and is amplified by the driver MCP1305. Resistor R_L limits collector current and resistor R_G limits the maximum current of the gate of the tested IGBT. In the measurement set-up the oscilloscope Rigol DS1052E, the current probe Tektronix TCPA 300, the feeder NDN of the type DF1760SL10A and the functional generator of the type NDN JC5603P are used. The case temperature of the investigated device is measured by the pyrometer Optex PT-3S. The band of the applied oscilloscope is 50 MHz, and the current probe −100 MHz. The applied driver is characterised with the maximum output current of 4.5 A and with the maximum output voltage amounting to 18 V. During measurements the investigated transistor is situated in the thermostat.

Investigations were performed for type the IRG4PC40UD transistor [28] manufactured by International Rectifier company. During measurements this transistor was screwed to a large aluminium heat-sink situated in the thermostat. The gate of this transistor was controlled by a rectangular pulses train. The amplitude of this signal was equal to 15 V, whereas its frequency was equal to 20 kHz. Resistor R_G of resistance equal to 210 Ω was connected in series with the gate of the transistor. In order to minimise influence of a self-heating phenomenon on the investigated waveforms, all the measurements presented in this section were obtained just after switching-on or switching-off the control signal.

In Figure 5 influence of temperature on the measured waveforms of collector current obtained at selected temperature values in the range from 21 to 114 °C is shown. Such a range of investigations was selected arbitrarily taking into account three reasons. Firstly, the lowest value of temperature should be equal to typical room temperature. Secondly, the highest value of temperature must be lower than the maximum allowable temperature of operation of the considered transistor. Thirdly, differences between the highest and lowest temperature should be possibly big to visibly illustrate influence of temperature on dynamic properties of the tested transistor.

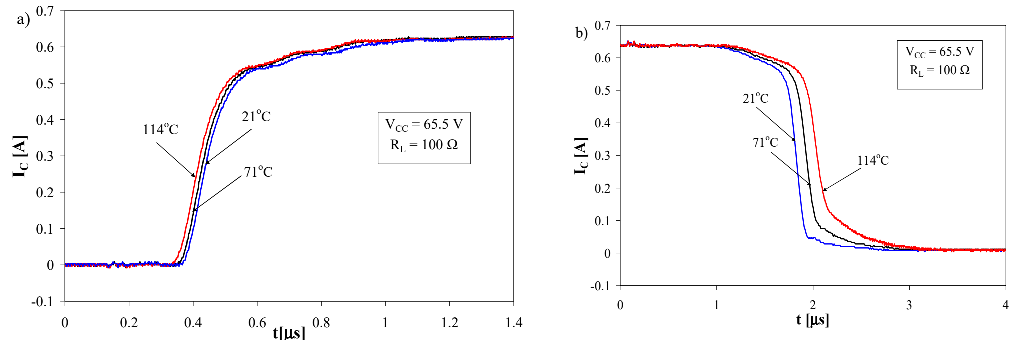

Figure 5. Measured waveforms of collector current of the considered transistor in (**a**) switching-on and (**b**) switching-off the IGBT at different values of temperature.

During measurements, the collector circuit of the tested IGBT was fed from the source V_{CC} of constant voltage equal to 65.5 V Resistor R_L of resistance 100 Ω which was connected between this source and the collector of the tested transistor. As it is visible, temperature very weakly influences waveforms $I_C(t)$ while switching-on, whereas influenced of temperature on these waveforms was strong while switching off. In particular, considerable extension of the so-called current tail could be observed at a temperature rise. The temperature rise caused acceleration of the switching-on process of the investigated transistor by 50 ns and a slowdown of the switching-off process of this transistor by almost 500 ns.

Using the presented in the previous section dynamic model of the IGBT, waveforms of voltages and currents of the considered device during the switching process at fixed values of temperature were computed. The results of computations obtained using the authors' new model are presented in Figures 6–8 as red lines. They are compared with the results of measurements (points) and the results of computations obtained by means of two popular literature models—the Hefner model [27,29] built-in in the SPICE (black lines) and the model available at the website of International Rectifier [15] (blue lines).

The considered literature models were described in detail in paper [16]. Figure 6 shows waveforms of collector current during the switching-off process of the considered device supplied in the identical manner as in the case considered in Figure 5. The results shown in Figure 6a correspond to temperature equal to 22 °C, whereas the results shown in Figure 6b correspond to temperature equal to 114 °C.

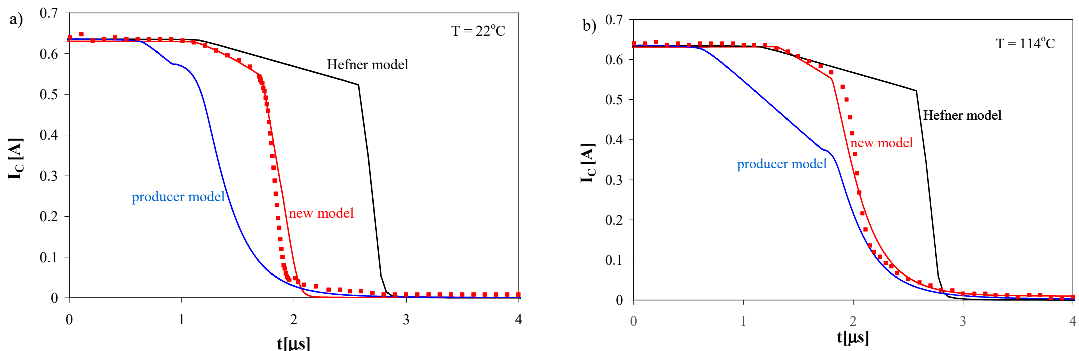

Figure 6. Computed and measured waveforms of collector current during the switching-off process at temperature equal to (**a**) 22 °C and (**b**) 114 °C.

As it is visible, good agreement was obtained between the results of computations and measurements at both the considered values of temperatures only for the authors' model. For the producer model [15], the switching-off process ran too quickly, especially for temperature T = 22 °C. In temperature equal to 114 °C, essential improvement in accuracy of computations performed with the described model within the range of current values below 300 mA could be observed. In turn,

the results of computations obtained with the use of the Hefner model were characterised by the overlong switching-off process. Similarly, as it was presented for dc characteristics in paper [16], this model does not take into account influence of temperature on the shape of characteristics of the considered device.

Figure 7 shows waveforms of collector current of the investigated IGBT during the switching-on process for temperature equal to 22 °C (Figure 7a) and 114 °C (Figure 7b).

At temperature equal to 22 °C good agreement between the results of measurements and computations was obtained for all the tested models. In contrast, for temperature T = 114 °C good agreement between the results of computations and measurements was obtained with the use of the authors' model, and acceptable agreement between these results was assured also by the literature models. The producer model is characterised by good accuracy only within for values of collector current below 300 mA.

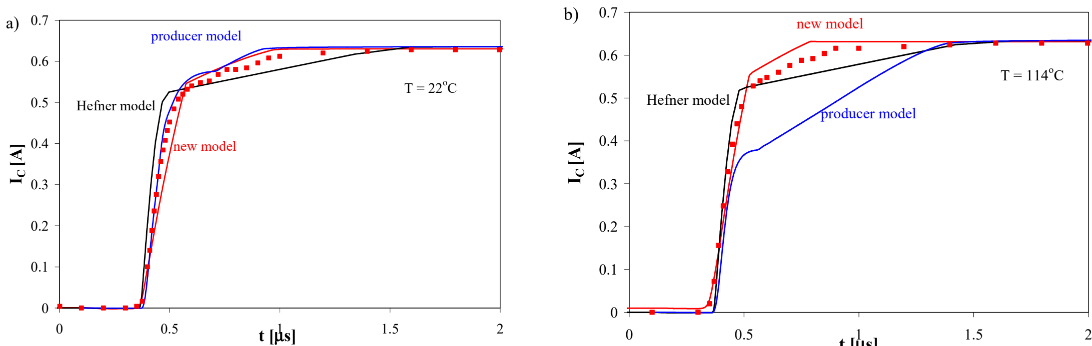

Figure 7. Measured and computed waveforms of collector current while switching-on at temperature equal to (**a**) 22 °C and (**b**) 114 °C.

Figure 8 illustrates waveforms of collector current during the switching-on process (Figure 8a) and the switching-off process (Figure 8b) of the tested IGBT operating at room temperature and load resistance R_L equal to 14.7 Ω.

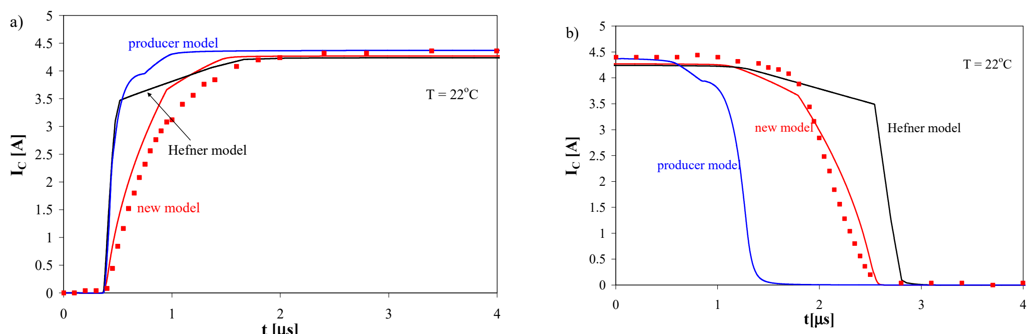

Figure 8. Measured and computed waveforms of collector current while (**a**) switching-on and (**b**) switching-off at R_L = 14.7 Ω.

Only for a new model good agreement between the results of measurements and computations was obtained. Computations performed with the use of both the literature models showed incorrectly too short duration time of the switching-on process. In turn, the computed with the use of these models waveform of collector current during the switching-off process showed too short duration time of this process for the producer model and too long—for the Hefner model.

Comparing the results of measurements and computations obtained for different values of load resistance (Figures 6a, 7a and 8), it is visible that at a higher value of this resistance both the considered switching times are shorter than for a lower value of resistance R_L.

Table 1 shows the values of times t_{on} and t_{off} computed with the use of three considered models and measured values which correspond to different values of resistance R_L and temperature. As one can notice, in five out of six considered cases the value of the mentioned times was computed with the use of the author's model. In the case of time t_{off} computed at temperature 114 °C and resistance R_L = 100 Ω the value of this time was obtained with the use of the producer model. However, as it is visible in Figure 6b, this model does not describe exactly the whole course of collector current during the switching-off process, so the accurately computed value of time t_{off} results from good modelling of the coordinates of only two points in the waveform $I_C(t)$ used in computing values of parameters shown in this table.

Table 1. Computed and measured values of times t_{on} and t_{off}.

R_L[Ω]	T_a[°C]	t_{on}[ns]				t_{off}[ns]			
		Producer Model	Hefner Model	Authors' Model	Measured	Producer Model	Hefner Model	Authors' Model	Measured
100	22	525	794	560	618	1736	2722	1882	1880
100	114	1033	808	460	566	2312	2725	2243	2370
14.7	22	542	870	1072	1336	1295	2592	2460	2236

As it visible in the presented comparison of the results of computations and measurements (Table 1), only the authors' model assured good accuracy. The computed by means of both literature models waveforms of collector current while switching significantly differ from the results of measurements. The proposed model is correct over a wide range of changes of temperature and load resistance.

As it can be observed, the literature models assured good agreement between the results of computations and measurements only in the case of the process of switching-on at room temperature. In other operating conditions visible differences between the results of computations and measurements were observed. In turn, the authors' model correctly described influence of temperature on waveforms of collector current both while switching-on and switching-off the transistor.

Using the authors' model, waveforms of the collector current while switching-off (Figure 9) and switching-on (Figure 10) the considered transistor are computed and the obtained results of computations are compared to the results of measurements.

In Figure 9 it is visible that the time of switching-off increases together with an increase of the switched current. In the investigated range of current i_C values, time of switching-off increases from 1.22 μs to 2.34 μs. This increase is linear and time of switching-off increases with an increase of current with the slope equal to about 94 ns/A.

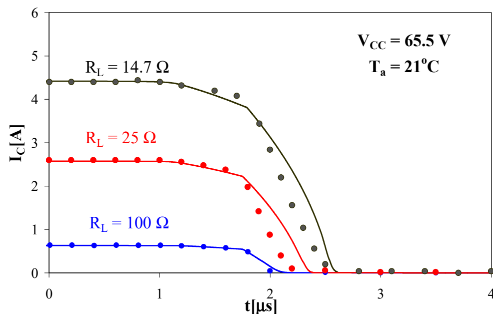

Figure 9. Computed and measured waveforms of current i_C while switching-off the transistor.

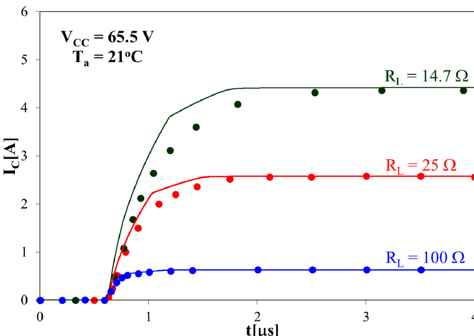

Figure 10. Computed and measured waveforms of current i_C while switching-on the transistor.

In Figure 10 it is visible that the on-time increases together with an increase of the switched current. In the investigated range of values of currents i_C, the on-time increases from 620 ns to 1.69 µs. This increase is linear, and the on-time increases with an increase of current of 186 ns/A. This increase is double compared to the case of switching-off.

From the point of view of switched-mode electronic circuits energy losses during the switching process are essential. In Figures 11 and 12 the computed and measured waveforms of power losses in the investigated transistor at two different values of temperature are presented. Figure 11 shows a shift between the maxima of courses p(t) obtained while switching-off in the considered temperatures, whereas the corresponding waveforms p(t) while switching-on shown in Figure 12 differs between one another imperceptibly.

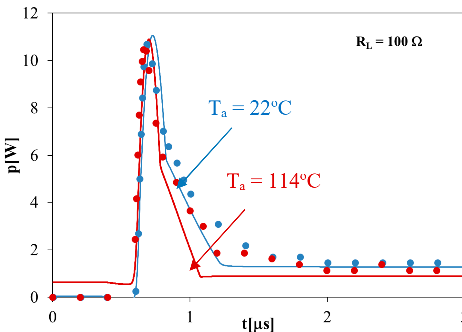

Figure 11. Measured and computed waveforms of power dissipated in the transistor while switching-on.

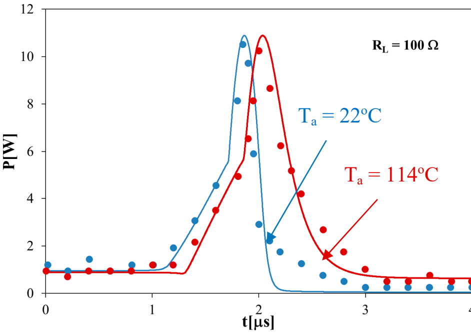

Figure 12. Measured and computed waveforms of power dissipated in the transistor while switching-off.

In Figure 13 the computed and measured waveforms of gate-emitter voltage while charging the gate of the investigated transistor are presented. These waveforms were measured and computed for collector current I_C = 20 A and voltage feeding the collector V_{CC} = 400 V. Current of the gate during the test amounted to 100 mA. As it is visible, the results of computations and measurements are convergent

and satisfactory; the differences between them do not exceed 10%. This confirms correctness of the description of input capacitance of the considered transistor.

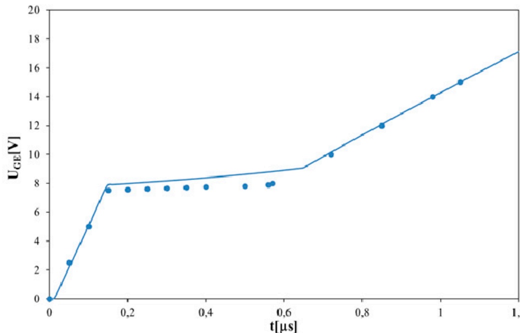

Figure 13. Computed and measured waveforms of gate-emitter voltage while charging the gate of the transistor.

4. Conclusions

In this article a new form of the IGBT model dedicated for the SPICE software is proposed. This model takes into account influence of temperature on dynamic properties of the considered device. In the description of the proposed model new dependences of device parasitic capacitances on temperature and on the co-ordinates of the device operating point are included in the form of analytical formulas.

The usefulness of the elaborated model is verified for the transistor operating as a switch. Waveforms of collector current are computed with the use of the new model and two models given in the literature. Computations are performed at different values of temperature and load resistance. The results of computations are compared to the results of measurements. The waveforms of collector current while switching-on and switching-off obtained using the new model fit well the results of measurements in the whole considered range of changes of temperature and load resistance. In contrast, the results of computations obtained using the considered literature models visibly differ from results of measurements. The difference increase while load resistance decreases.

The performed computations and measurements prove correctness of the new model. It is also visible that temperature strongly influences the value of off-time, but its influence on on-time could be omitted. Moreover, it is also shown that the new model properly describes waveform of power dissipated in the investigated transistor while it is being switched. Correctness of the used description of the transistor input capacitance prove good agreement between the computed and measured waveforms of gate-emitter voltage while charging the gate.

The disadvantage of the proposed model is a complicated description of internal capacitances making use of splines. It could result in some problems with convergence of the analysis performed for a long time—equal to hundreds or thousands of periods of the signal controlling the gate of the considered transistor.

The presented dynamic model of the IGBT could be useful for designers of power electronics circuits, making possible realisation of more accurate computer simulation of such circuits. This model could be also useful in didactics to present influence of temperature changes on switching-on and switching-off processes in power converters including IGBTs.

As it is commonly known, temperature of the IGBT could change as a result of self-heating phenomena [17]. Therefore, in further investigations the authors will elaborate an electrothermal model of the IGBT on the basis of the dynamic model presented in this article.

Author Contributions: The measurements presented in this manuscript and their evaluation was carried out by P.G. Manuscript was prepared and the equations were formulated by P.G. and K.G. Finally, K.G. supervised the research.

Funding: The scientific work was financed with the Polish science budget resources in the years 2017–2021, as the investigation project within the framework of the program "Diamentowy Grant". The project was financed within the program of the Ministry of Science and Higher Education called "Regionalna Inicjatywa Doskonałości" in the years 2019–2022, the project number is 006/RID/2018/19, the sum of financing is 11 870 000 PLN.

Conflicts of Interest: The authors declare no conflict of interest.

References

1. Baliga, B.J.; Adler, M.S.; Love, R.P.; Gray, P.V.; Zommer, N.D. The insulated gate transistor—A new 3-terminal MOS-controlled bipolar power device. *IEEE Trans. Electron Devices* **1984**, *31*, 821–828. [CrossRef]
2. Ericson, R.; Maksimovic, D. *Fundamentals of Power Electronics*, 2nd ed.; Kluwer Academic Publisher: Norwell, MA, USA, 2001.
3. Rashid, M.H. *Power Electronic Handbook*, 2nd ed.; Academic Press: Oxford, UK, 2007.
4. Kazimierczuk, M.K. *Pulse-width Modulated DC-DC Power Converters*, 2nd ed.; John Wiley & Sons: Hoboken, NJ, USA, 2008.
5. Maksimovic, D.; Stankovic, A.M.; Thottuvelil, V.J.; Verghese, G.C. Modelling and simulation of power electronic converters. *Proc. IEEE* **2001**, *89*, 898–912. [CrossRef]
6. Mohan, N.; Robbins, W.P.; Undeland, T.M.; Nilssen, R.; Mo, O. Simulation of Power Electronic and Motion Control Systems—An Overview. *Proc. IEEE* **1994**, *82*, 1287–1302. [CrossRef]
7. Rashid, M. *SPICE for Power Electronics and Electronic Power*, 3rd ed.; Taylor and Francis Group: Oxfordshire, UK, 2016.
8. Wilamowski, B.M.; Jaeger, R.C. *Computerized Circuit Analysis Using SPICE Programs*, 1st ed.; McGraw-Hill: New York, NY, USA, 1997.
9. Górecki, K.; Zarębski, J. Influence of MOSFET model form on characteristics of the boost converter. *Inf. MIDEM* **2011**, *41*, 1–7.
10. Bargieł, K.; Zarębski, J.; Bisewski, D. SPICE-aided modeling of high-voltage silicon carbide JFETs. In *IOP Conference Series: Materials Science and Engineering*; IOP Publishing Ltd.: Bristol, UK, 2016; Volume 104. [CrossRef]
11. Hefner, A.R.; Diebolt, D.M. An experimentaly verified IGBT model implemented in the Saber circuit simulator. *IEEE Trans. Power Electron.* **1994**, *9*, 532–542. [CrossRef]
12. Baliga, B.J. Analytical modelling of IGBTs: Challenges and solutions. *IEEE Trans. Electron Devices* **2013**, *60*, 535–543. [CrossRef]
13. Apeldoorn, O.; Schmitt, S.; De Doncker, R.W. An electrical model of a NPT-IGBT including transient temperature effects realized with PSpice device equations modeling. In Proceedings of the IEEE International Symposium on Industrial Electronics, Guimaraes, Portugal, 7–11 July 1997; pp. 223–228.
14. Wu, R.; Wang, H.; Pedersen, K.B.; Ma, K.; Ghimire, P.; Iannuzzo, F.; Blaabjerg, F. A temperature-dependent thermal model of IGBT modules suitable for circuit-level simulations. *IEEE Trans. Ind. Appl.* **2016**, *52*, 3306–3314. [CrossRef]
15. Spice Models and Saber Models. Web-Site of International Rectifier. Available online: http://www.irf.com/product-info/models/saber/ (accessed on 4 February 2019).
16. Górecki, P.; Górecki, K.; Zarębski, J. Modelling the temperature influence on dc characteristics of the IGBT. *Microelectron. Reliab.* **2017**, *79*, 96–103. [CrossRef]
17. Górecki, K.; Górecki, P. Modelling the influence of self-heating on characteristics of IGBTs. In Proceedings of the 21st International Conference Mixed Design of Integrated Circuits and Systems MIXDES, Lublin, Poland, 19–21 June 2014; pp. 298–302.
18. Sheng, K.; Williams, B.W.; Finney, S.J. A review of IGBT models. *IEEE Trans. Power Electron.* **2000**, *15*, 1250–1266. [CrossRef]
19. Górecki, K.; Górecki, P. Modelling dynamic characteristics of the IGBT with thermal phenomena taken into account. *Microelectron. Int.* **2017**, *34*, 160–164. [CrossRef]
20. Liu, Y.T.; Liang, S.Q.; Jin, D.H.; Peng, J.C. Performance comparison of Si IGBT and SiC MOSFET power devices based LCL three-phase inverter with double closed-loop control. *IET Power Electron.* **2019**, *12*, 322–329. [CrossRef]

21. Seo, J.H.; Choi, C.H.; Hyun, D.S. A new simplified space-vector PWM method for three-level inverters. *IEEE Trans. Power Electron.* **2001**, *16*, 545–550.
22. Blaabjerg, F.; Jaeger, U.; Munknielsen, S.; Pedersen, J.K. Power Losses in PWM-VSI Inverter Using NPT or PT IGBT Devices. *IEEE Trans. Power Electron.* **1995**, *10*, 358–367. [CrossRef]
23. Górecki, P. Investigation of the influence of thermal phenomena on dynamic parameters of the IGBT. In Proceedings of the 25th International Conference on Mixed Design of Integrated Circuits and Systems MIXDES, Gdynia, Poland, 21–23 June 2018; pp. 243–247.
24. Avenas, Y.; Dupont, L.; Khatir, Z. Temperature Measurement of Power Semiconductor Devices by Thermo-Sensitive Electrical Parameters—A Review. *IEEE Trans. Power Electron.* **2012**, *27*, 3081–3092. [CrossRef]
25. Górecki, P.; Górecki, K. Modelling influence of temperature on the switching process of IGBTs. In Proceedings of the 24th International Workshop on Thermal Investigations of ICs and Systems Therminic 2018, Stokholm, Sweden, 26–28 September 2018. [CrossRef]
26. Napieralski, A.; Napieralska, M. *Polowe Półprzewodnikowe Przyrządy Dużej Mocy*, 1st ed.; Wydawnictwa Naukowo-Techniczne: Warsaw, Poland, 1995.
27. Hefner, A.R. An investigation of the drive circuit requirements for the power insulated gate bipolar transistor (IGBT). *IEEE Trans. Power Electron.* **1991**, *6*, 208–219. [CrossRef]
28. IRG4PC40UD Insulated Gate Bipolar Transistor with Ultrafast Soft Recovery Diode, Data Sheet, International Rectifier. 1997. Available online: https://www.infineon.com/dgdl/irg4pc40udpbf.pdf?fileId=5546d462533600a4015356442ac722dc (accessed on 15 May 2019).
29. PSpice A/D Reference Guide. Product Version 15.7. 2006. Available online: siyh.byethost11.com/PDF/PSpiceGuide.pdf?i=1 (accessed on 15 May 2019).

© 2019 by the authors. Licensee MDPI, Basel, Switzerland. This article is an open access article distributed under the terms and conditions of the Creative Commons Attribution (CC BY) license (http://creativecommons.org/licenses/by/4.0/).